Journal of Applied Fluid Mechanics, Vol. 12, Special Issue, pp. 19-28, 2019.
Selected papers from *17th International Days on Heat Transfer* ***(JITH-2017)****, 2017*
Available online at www.jafmonline.net, ISSN 1735-3572, EISSN 1735-3645.
DOI: 10.36884/jafm.12.SI.29917

Effect of Replacement of Air N_2 by H_2O on Internal Structure and Pollutants Formation in an Opposed Jet Diffusion Combustion of a Hydrogenated Biogas in Flameless Regime

A. Hadef [1†], A. Mameri[1], Z. Aouachria[2] and F. Tabet[3]

[1] *Mechanical Engineering Department, University Larbi BEN MHIDI, PB 385, 04000, Algeria.*
[2] *Applied Physical Energetics Laboratory, University Batna1 05000, Algeria.*
[3] *LCGE (Gaseous Fuels and Environment Laboratory), Sciences and Technology University of Oran, BP 1505 El Menaouer Oran 31000, Algeria.*

† *Corresponding Author Email: hadef_am@yahoo.fr*

(Received March 30, 2018; accepted June 25, 2018)

ABSTRACT

Nowadays, combustion intervenes in more than 80% of primary energy consumption, the control of the combustion process is essential. Fuel consumption, emissions reduction and energetic efficiency increasing are challenges to which researchers are faced. The most interesting invention that meets nearly all these prerequisites is the flameless combustion regime. This regime is based on the dilution and preheating of reactants by recirculated exhaust gases. This regime is well adapted for the low calorific fuels such as biofuels. In this context, this work presents a contribution to flameless combustion which differs from the conventional one by its low emissions and high efficiency. This numerical study considers the effects of air contained nitrogen substitution by water vapor, the oxygen volume concentration in the oxidizer stream and hydrogen doping of the fuel. To simplify analysis, the opposed jet configuration is adopted with a full diffusive transport approach. The MILD combustion is described by the well-known Gri 3.0 mechanism. It has been noticed that oxygen reduction within a range of 4% to 6%, which is a characteristic of flameless combustion, reduces significantly temperature and emissions whereas hydrogen addition to the fuel, which increases temperature and emissions, has a lower impact. Dilution by water vapor reduces temperature and emissions by thermal and chemical effects except OH radical.

Keywords: Hydrogenated biogas; Dilution by H_2O; Flameless combustion; Thermal and chemical effects of H_2O.

NOMENCLATURE

a	strain rate	Y_O	feed stream mass fraction of the oxygen
C_p	specific heat at constant pressure		
D_Z	diffusion coefficient	λ	thermal conductivity
Hi	enthalpy of species i	v_F	speeds of the fuel cm
Le	Lewis number		
LHV	Lower Heating Value	v_0	speeds of the oxidant cm
		P	operating pressure
T_∞	temperature of the radiating substance	ρ	density
T	temperature	q_r	radiative heat loss W
Y_k	mass fraction of species	σ	stefan-Boltzmann constant
Y_F	feed stream mass fraction of the fuel		

1. INTRODUCTION

Conventional combustion produces emissions such as carbon monoxide (CO), carbon dioxide (CO_2) and nitric oxides (NOx) which are harmful for the human being and biosphere, moreover, carbon dioxide is a greenhouse gas. With population growth, fuel consumption increased considerably which amplifies combustion emission effects. To minimize harmful emissions, restrictive regulations are issued, several works are devoted to enhancing the combustion process. A new combustion regime was discovered by Wunning *et al.* (1991) in Germany; it is named FLameless Oxidation (FLOX) of MILD combustion. In this regime no visible flame is detected, it is stable with uniform property fields and with very low (CO and NO) emissions. To meet the MILD or FLOX regime, it is necessary to dilute fuel and oxidizer jets with a strong recirculation of flue gases before reaction so that oxygen concentration is very low, Peng Fei *et al.* (2011). In an opposed jet configuration, De Joannon *et al.* (2009, 2012a, b) studied the characteristics of the diffusion MILD combustion of CH_4+N_2/air where they evaluated numerically the temperature distribution and the heat release in function of several parameters. FLOX regime boundaries and the reaction zone structure of a nitrogen diluted methane with a highly preheated oxidizer was studied by Maruta *et al.* (2000). Results showed that extinction limits expanded with air preheating temperature, moreover, when this temperature exceeded 1300K the extinction limits vanished. The impact of the preheating air temperature and oxygen concentration reduction in the oxidizer on the NOx formation in an opposed jet diffusion combustion were studied by Fuse *et al.* (2009). The authors used the well-known Gri 3.0 mechanism to describe MILD combustion kinetics and NOx formation, results were confronted experimentally. Mohamed et al. (2009) showed that NOx mass fraction is sharply reduced in flameless regime when diluting methane by nitrogen. Zhang *et al.* (2015) studied the diluent effect on the self-ignition temperature and the total reaction rates in both conventional and FLOX combustion regimes.

Mameri *et al.* (2018) have studied the influence of several operating conditions (biogas composition, hydrogen enrichment and oxidizer dilution) on MILD combustion structure and emissions in an opposed jet. Attention is paid to the chemical effect of added CO_2 to the oxidizer. It has been noticed that oxygen reduction in the oxidizer side has a significant effect on temperature and emissions while hydrogen addition is less significant. Combustion temperature and emissions are considerably reduced by oxygen reduction in the oxidizer and augmented by hydrogen increasing in the fuel. Temperature maximums and species are not influenced by biogas composition in MILD combustion of biogas. In the same context Hadef *et al.* (2018) numerically studied the effect of water vapor addition to the biogas in MILD combustion in an opposed jet diffusion configuration. Composition of biogas was 75% CH_4 and 25% CO_2, strain rate $120s^{-1}$ and pressure 1 atm. The results show that dilution by H_2O reduces the formation of thermal NO, CO and CO_2. Soot precursor namely CH_2O is also reduced by H_2O addition whereas C_2H_2 is increased by H_2.

Flameless combustion is known for its ability to reduce emissions such as carbon monoxide, nitric oxides NOx, carbon dioxide (CO_2), unburnt particles and soot which are primary pollutants Derudi *et al.* (2007). In the combustion process, fuel carbon is transformed in successive chemical reactions to CO_2 and CO whereas NOx are produced when combustion temperature exceeds 1700K. Under these constraints, it is necessary to find a substitution, several solutions were considered among which the use of renewable energies like solar and wind energy, however they are intermittent and inefficient.

The use of biogas, a renewable energy, which is naturally diluted by CO_2 gives significant advantages, environmental and economical, compared to other fuels. This means that biogas containing methane have a low CO_2 emission level compared to hydrocarbon since its carbon/hydrogen ratio is slow. Moreover, the use of the biogas in lean combustion systems can also reduce NOx, unfortunately; its flame is weak and unstable, for that reason hydrogen is used to give more reactivity and to stabilize the flame. Many studies handled the case of hydrogen doped mixtures of biogas-air under several conditions Mameri *et al.* (2016).

2. GEOMETRY AND MATHEMATICAL FORMULATION

The two opposed jets configuration (Kee *et al.*, 1988) is adopted in this study, the first jet is composed by fuel, the second injects oxidizer (Fig. 1). This geometry facilitates the laminar flame structure study, since it permits important simplifications of the flow equations. In this configuration, the reaction zone develops in a stable diffusion layer, this makes the flow steady and unidimensional in *y* direction.

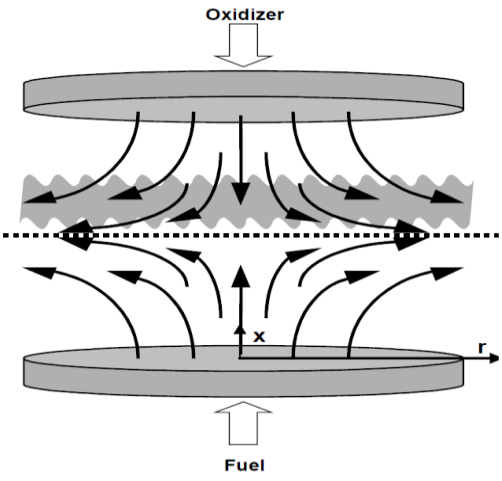

Fig. 1. Geometry of opposed jet configuration.

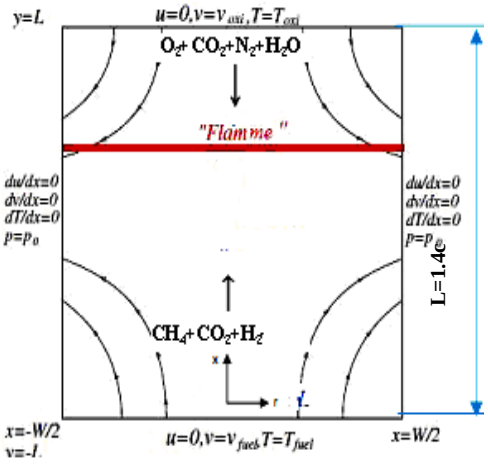

Fig. 2. Boundary conditions of an opposed jet configuration.

The schematic representation of the flow is given in Fig. 2, the fuel is a hydrogen doped biogas BG75 (75% CH_4+ 25 CO_2) and the oxidizer is a preheated air diluted by water vapor. The distance between the two jets is L = 1.4 cm, the strain rate is a = 120 s^{-1} and is kept constant by calculating injection velocities of both oxidizer and fuel, $v_0 = v_F$ from Eq. (1) (Fisher *et al.*, 1997); the pressure is constant and equal to 1 atm.

$$a = \frac{2(-v_0)}{L}\left[1+\frac{v_F}{(-v_0)}\sqrt{\frac{\rho_F}{\rho_0}}\right] \tag{1}$$

Where v_O , v_F , ρ_O and ρ_F are respectively the oxidizer injection velocity (which is equal to the one of the fuel), fuel injection velocity, oxidizer density and fuel density. The fuel is injected at a temperature of T_F =300 K and the oxidizer at T_O =1200 K. Biogas is composed by 75% of methane and 25% of CO_2 and doped by a volume of hydrogen ranging from 10% to 30%. The fuel composition is given by:

$$0.75(1-\alpha)CH_4 + 0.25(1-\alpha)CO_2 + \alpha H_2 \tag{2}$$

The oxidizer is composed by a volume of 4% oxygen, 17% of carbon dioxide and two varied fractions of nitrogen and water vapor, the volumetric composition is given by:

$$0.04O_2 + 0.17CO_2 + (0.79-\beta)N_2 + \beta H_2O \tag{3}$$

Where α, β are numbers of moles of H_2 and H_2O added to biogas.

The Chemkin program (2013) is used to solve the governing Eqs. (4) – (6) with the boundary conditions (8)

$$H - 2\frac{d}{dx}\left(\frac{FG}{\rho}\right) + \frac{3G^2}{\rho} + \frac{d}{dx}\left[\mu\frac{d}{dx}\left(\frac{G}{\rho}\right)\right] = 0 \tag{4}$$

Where $H=\frac{1}{r}\frac{dP}{dr}$, $G(x)=-\frac{\rho v}{r}$ and $F(x)=\frac{\rho u}{r}$

$$\rho u\frac{dY_k}{dx} + \frac{d}{dx}(\rho V_k Y_k) - \omega_k W_k = 0 \tag{5}$$

$$\rho u\frac{dT_k}{dx} - \frac{1}{C_p}\frac{d}{dx}\left(\lambda\frac{dT}{dx}\right) + \frac{\rho}{C_p}\sum_k C_{pk}V_k Y_k\frac{dT}{dx} - \frac{1}{C_p}\sum_k h_k\omega_k - \frac{q_r}{C_p} = 0 \tag{6}$$

With

$$G(x) = \frac{dF(x)}{dx} \tag{7}$$

Boundary conditions for the fuel (F) and the oxidizer (O) are:

$$x = 0 : F = \frac{\rho_F u_F}{2}; G = 0; T = T_F; \quad \rho u Y_F + \rho Y_k V_k = (\rho u Y_k)_F \tag{8}$$

$$x = L : F = \frac{\rho_0 u_O}{2}; G = 0; T = T_0; \quad \rho u Y_F + \rho Y_k V_k = (\rho u Y_k)_O \tag{9}$$

3. COMPUTATIONS DETAILS

The set of differential equations which governs the flow are solved by assuming that each species diffuses with a different velocity, this implies that Lewis number is not constant. Heat loss by radiation is modeled by the optical thin model, radiating species are CO_2, H_2O, CO, and CH_4.

$$q_r = -4\sigma K_p\left(T^4 - T_\infty^4\right) \tag{10}$$

With

$$K_p = \sum_{i=1}^{4} P_i K_i \quad ; i = CO_2, H_2O, CO, CH_4 \tag{11}$$

Where σ is the Stefan-Boltzmann constant, T and T_∞ are respectively radiant substance temperature and ambient temperature, P_i is the partial pressure, K_i is the mean absorption coefficient of the species *i*. Chemical kinetics is described by the GRI 3.0 mechanism Smith *et al.* (2000), which is formed by 325 elementary reactions of 53 species.

4. RESULTS AND DISCUSSION

In this section, numerical procedure is validated and effects of different parameters on combustion structure are exposed and discussed.

4.1 Validation of the Numerical Procedure

The opposed jet configuration is largely used in numerical and experimental studies. Many fuels and oxidizers are tested (Smith *et al.*, 1995; Seungro *et al.*, 2015 and Sheng, 2011), this configuration simplifies flow equations and combustion structure. Unfortunately, there are no experimental results which used biogas in MILD combustion regime in this configuration, the validation is based on the work of Sung *et al.* (1995) which uses methane in conventional combustion. The experimental device is composed by two convergent nozzles of diameters of 1.4 cm and a distance between the jets

of 1.4 cm. Oxidizer is composed of 23% oxygen and 77% nitrogen, whereas fuel by methane; they are injected with a velocity of v = 25,5 cm / s, which corresponds to a train rate of a = 42 s^{-1}, ambient pressure is constant and equal to 1 atm.

In Fig. 4, a comparison between numerical computations and experiments are shown. Confrontation between temperature and major species namely CH_4, O_2, H_2O, CO_2 and CO show good agreement, also the maximum flame temperature is well reproduced that means that radiation losses are modeled accurately.

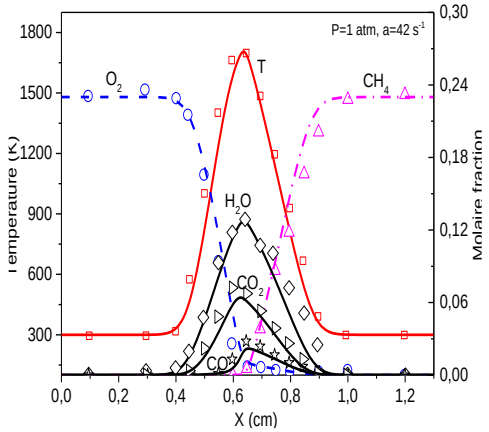

Fig. 4. Comparison between experience and computations (the symbols represent experimental results).

4.2 Radiation Effect

To illustrate the radiation effect in the combustion zone, the relative temperature is introduced (Park *et al.*, 2008):

$$f = \frac{(T_{nonrad} - T_{rad})}{T_{nonrad}} \tag{12}$$

where T_{nonrad} and T_{rad} are respectively the flame temperatures without and with radiation.

Profiles of the relative temperature of the BG75 biogas in atmospheric pressure are presented in Fig. 5. Figure 5(a) shows the effect of hydrogen doping (10% to 30%) on the relative combustion temperature, oxygen volume is 6% in the oxidizer. It can be seen that hydrogen addition to the fuel reduces the relative temperature since it is a low radiating gas. Whereas in Fig. 5(b), the relative temperature is increased by H_2O to the fuel, this is obvious because water vapor is a radiating species. Also, the substitution of CO_2 by the oxygen in the oxidizer side reduces relative temperature since CO_2 is a good radiating species (Fig. 5(c)).

4.3 Structure of the Combustion Zone

Figure 6 illustrates profiles of combined effects of the oxygen and hydrogen mole fraction variation in the oxidizer and in the fuel respectively. Combustion structure is presented by temperature, mole fractions of major and minor species. Maximum values of temperature, major and minor species are recorded near the position x = 1.1 cm. In Fig. 6(a) it is shown that when oxygen is reduced in the oxidizer stream, temperature is highly decreased, and its profile is shifted to the oxidizer side. The flameless combustion regime is specified by low oxygen concentration in the oxidizer (O_2 = 4 % to 6 %), which generates low temperature levels. When hydrogen is added to the fuel, the mixture becomes more reactive (hydrogen LHV=120 MJ/Kg) and the temperature increases with a shift of its profiles to the fuel side since hydrogen is a very diffusive species.

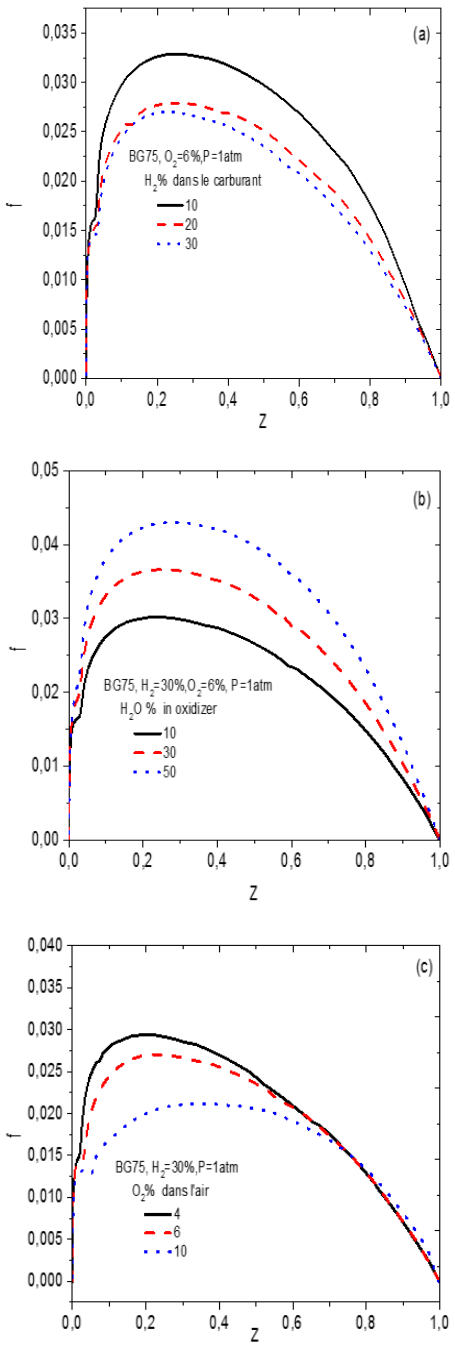

Fig. 5. Effect of addition H_2, H_2O and O_2 on relative temperature.

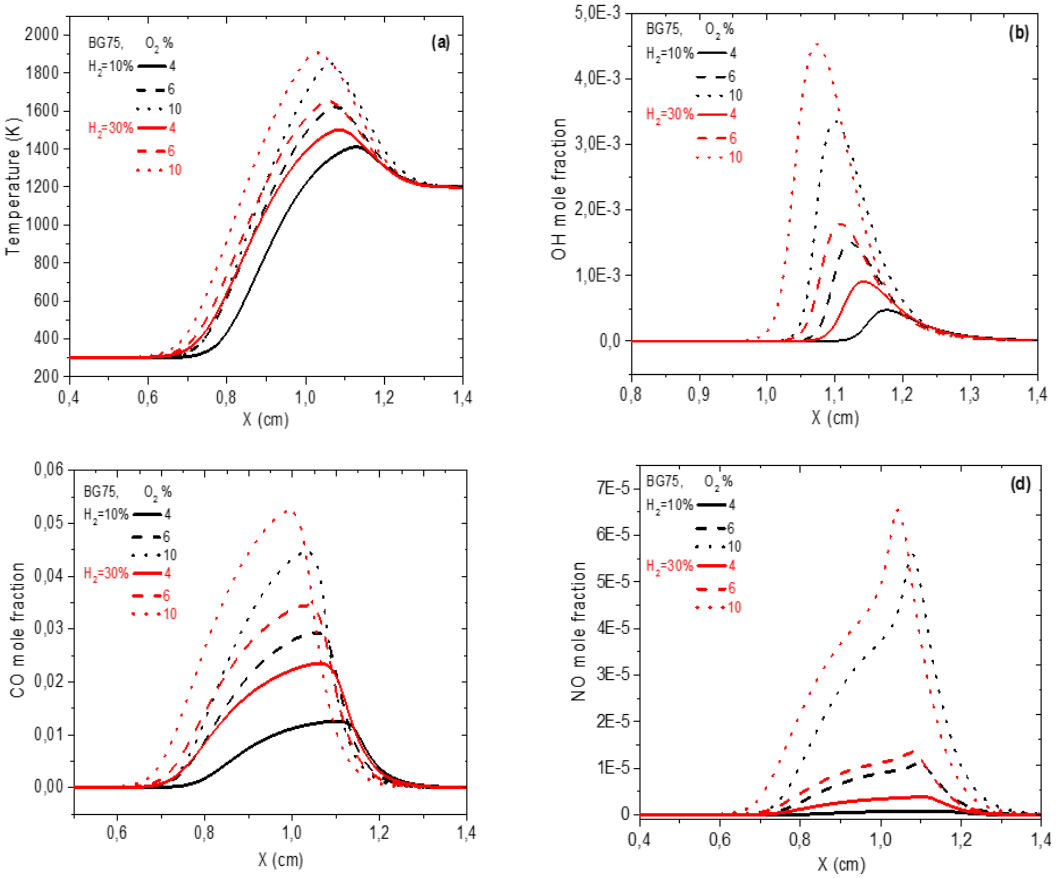

Fig. 6. Temperature, major and minor species evolution.

The minor species OH mole fraction is presented in Fig. 6(b); this species is reduced by oxygen reduction in the oxidizer and increased by hydrogen doping of the fuel. The OH species presents a slightly shifted profile to the oxidizer side relatively to temperature.

In Fig. 6(c), the mole fraction of CO is reduced by oxygen reduction in the oxidizer stream which induces a small shift of the profile to the oxidizer side. When oxygen is increased, the mixture becomes more reactive and the CO production increases.

The NO mole fraction is shown in Fig. 6(d), this species is considerably reduced by oxygen reduction, which is specific to MILD combustion (O2 = 4 % to 6 %) and slightly augmented by hydrogen addition to the fuel. In the specific conditions of the MILD combustion, the temperature decreases considerably which inhibits the NO formation. When the volume of oxygen increases in the oxidizer up to 10%, the temperature increases relatively, and NO is produced since the regime is similar to the conventional combustion.

Figure 7 illustrates maximum temperature variation in function of the ratio H_2O/N_2, N_2 being substituted by H_2O in the oxidizer stream. Oxygen volume is varied from 4% to 10%, hydrogen volume is kept constant and equal to 20% and strain rate $120s^{-1}$. When hydrogen volume is reduced from 10% to 4%, the temperature decreases from 1882K to 1471 with no effect of H_2O/N_2 ratio. On the other hand, when dilution by water vapor is applied, the maximum temperature reduces by 8.3% for 4% oxygen and by 4.04% for 10% O_2.

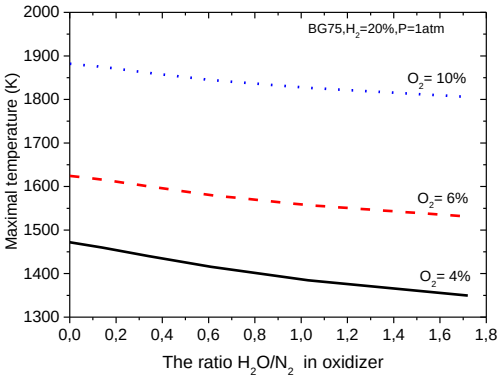

Fig. 7. Maximum temperature variation in function of H_2O/N_2.

Figure 8(a) illustrates OH mole fraction augmentation which is considerably affected by oxygen increasing in the oxidizer and hydrogen addition to the fuel. The OH species production is governed by the following elementary reactions Hwang *et al.* (2004) :

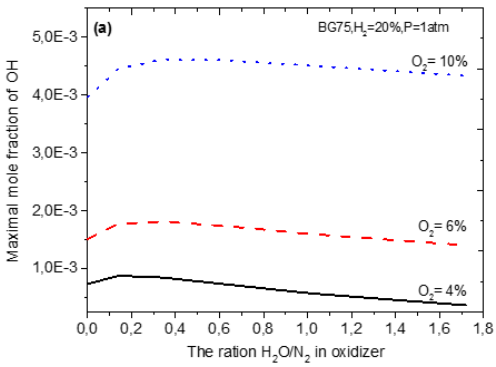
(a)
BG75,H2=20%,P=1atm
O2= 10%
O2= 6%
O2= 4%
Maximal mole fraction of OH
The ration H2O/N2 in oxidizer

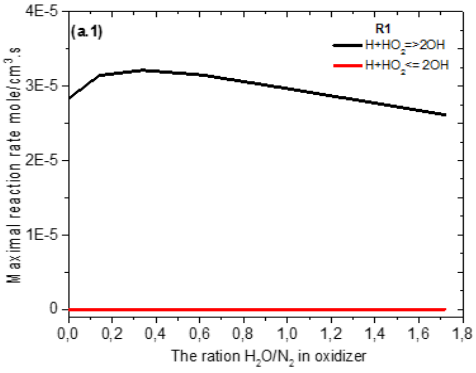
(a.1)
R1
H+HO2=>2OH
H+HO2<= 2OH
Maximal reaction rate mole/cm3.s
The ration H2O/N2 in oxidizer

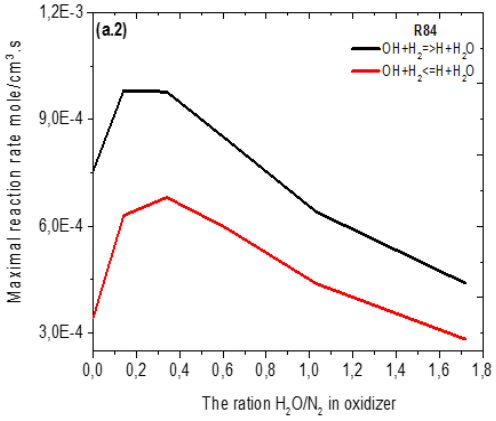
(a.2)
R84
OH+H2=>H+H2O
OH+H2<=H+H2O
Maximal reaction rate mole/cm3.s
The ration H2O/N2 in oxidizer

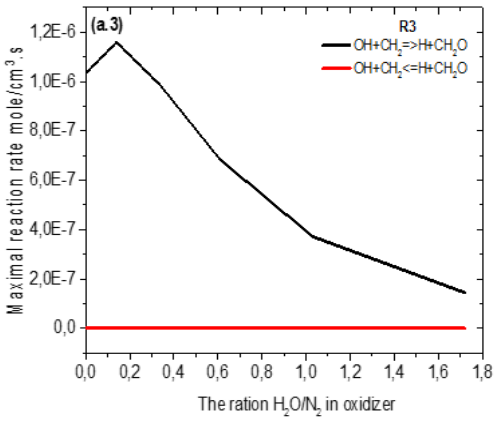
(a.3)
R3
OH+CH2=>H+CH2O
OH+CH2<=H+CH2O
Maximal reaction rate mole/cm3.s
The ration H2O/N2 in oxidizer

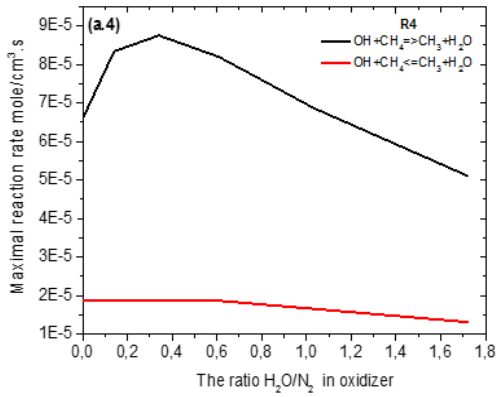
(a.4)
R4
OH+CH4=>CH3+H2O
OH+CH4<=CH3+H2O
Maximal reaction rate mole/cm3.s
The ratio H2O/N2 in oxidizer

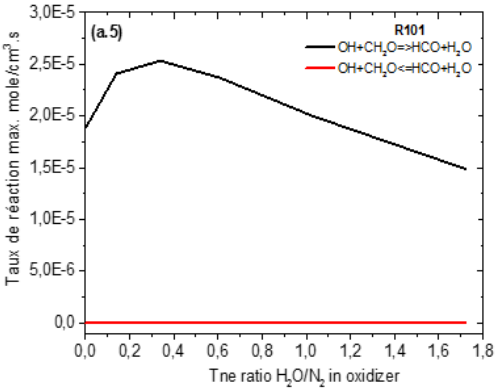
(a.5)
R101
OH+CH2O=>HCO+H2O
OH+CH2O<=HCO+H2O
Taux de réaction max. mole/cm3.s
Tne ratio H2O/N2 in oxidizer

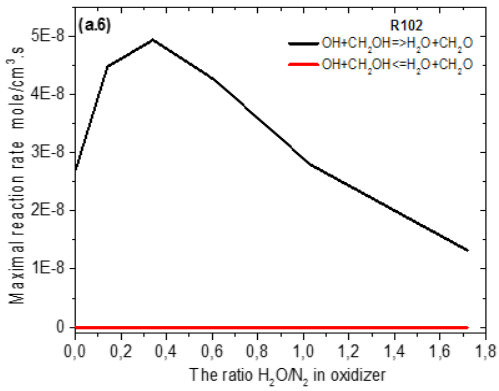
(a.6)
R102
OH+CH2OH=>H2O+CH2O
OH+CH2OH<=H2O+CH2O
Maximal reaction rate mole/cm3.s
The ratio H2O/N2 in oxidizer

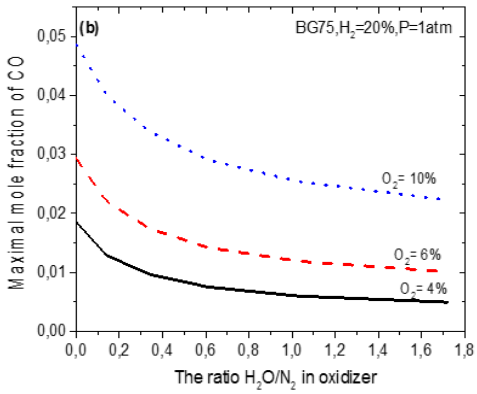
(b)
BG75,H2=20%,P=1atm
O2= 10%
O2= 6%
O2= 4%
Maximal mole fraction of CO
The ratio H2O/N2 in oxidizer

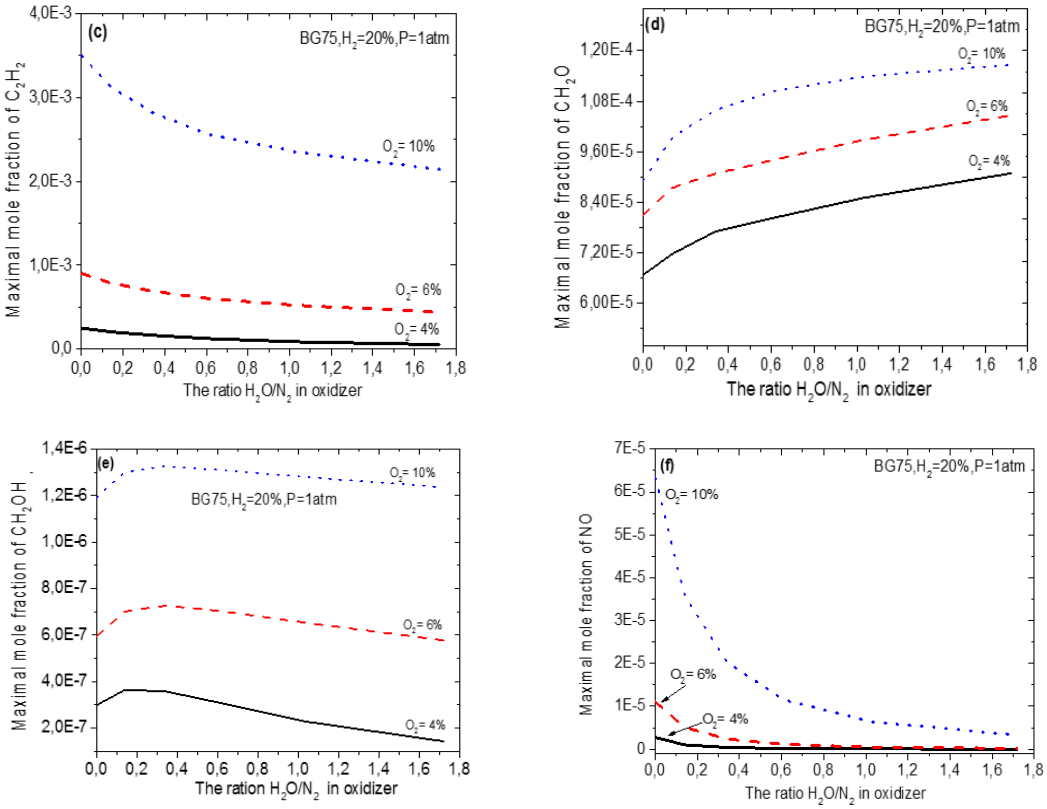

Fig. 8. Variation of the maximums of major and minor species mole fraction in function of H_2O/N_2.

R46	$H+HO_2$	$\Leftrightarrow 2OH$
R84	$OH + H_2$	$\Leftrightarrow H+H_2O$
R92	$OH + CH_2$	$\Leftrightarrow H+CH_2O$
R98	$OH+CH_4$	$\Leftrightarrow CH_3+H_2O$
R101	OH +CHO	$\Leftrightarrow HCO +H_2O$
R102	$OH +CH_2OH$	$\Leftrightarrow H_2O+CH_2O$

For 4% of oxygen volume, the production of OH species is dominated by the reaction (R46) Fig. 8(a.1), it follows a non-monotonic behavior, OH production reaches a maximum and then reduces gradually. The OH species is consumed in reactions R84, R92, R98, R101 and R101 showed in Fig. 8(a.2, 3, 4, 5, 6).

The variation of maximum CO mole fraction is presented in Fig. 8(b). This species is reduced by 61% with oxygen decreasing in the oxidizer stream from 10% to 4%, also, it is reduced with increasing H_2O/N_2 ratio. The species C_2H_2 and CH_2O are soot precursors whereas radicals OH and O can favorize soot oxidation and reduce its formation according to the following elementary reactions: $C_2H_2 + O \Leftrightarrow H + HCCO$ and $O + C_2H_2 \Leftrightarrow CO + CH_2$ (Liu *et al.*, 2001; Ruiz *et al.*, 2007; Chernov *et al.*, 2014 and Liu *et al.*, 2014)]. Increasing of C_2H_2 rate of formation is significantly enhanced by oxygen and reduced by H_2O dilution (Fig. 8(c)). The Fig. 8(d) illustrates the evolution of the maximum of the species CH_2O production rate when the ratio H_2O/N_2 varies from 0 to 1.72 and with a doping hydrogen volume of 20%. Dominant chemical reaction in the CH_2O species production are R3 and R6, moreover this species is highly affected by oxygen addition and H_2O dilution of the oxidizer (Glarborg et al. (2003). This species is principally produced from radical CH_2OH in a slightly exothermic step. It increases with oxygen increasing which is augmented by H_2O dilution (Fig. 8(e)). In Fig. 8(f), the maximum NO mole fraction is presented, when the oxygen volume is reduced in the oxidizer, the nitric monoxide falls drastically, it has a fraction of 2.7 ppm when hydrogen volume is 20%. Also, dilution by water vapor reduces the maximum of NO mole fraction by 98%.

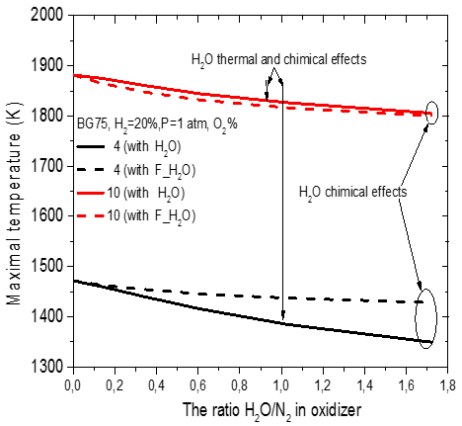

Fig. 9. Thermal and chemical effect of H_2O addition to the oxidizer on maximum temperature.

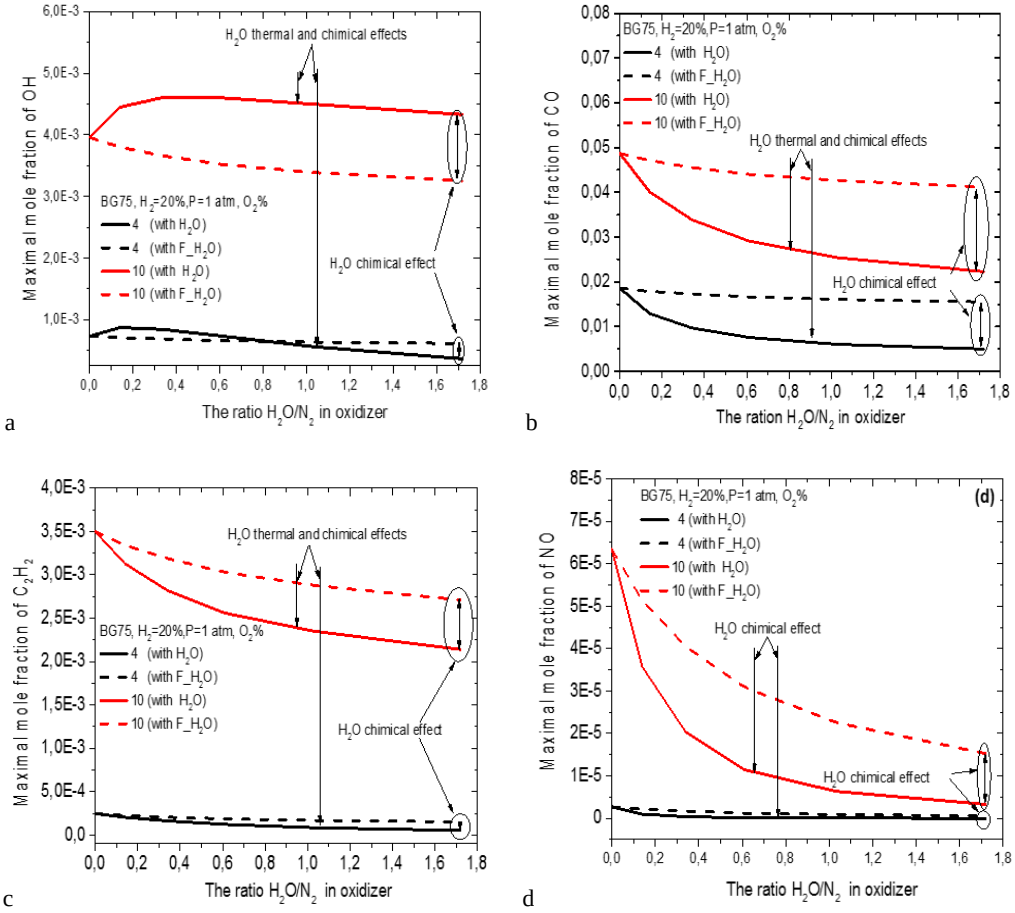

Fig. 10. Thermal and chemical effect of H_2O addition to the oxidizer on major and minor species.

4.4 Thermal and Chemical Effect of H_2O Addition to the Air

Figure 9 shows the effects (thermal and chemical) of H_2O addition in MILD combustion of a hydrogenated biogas. Here H_2O substitutes nitrogen with a molar ratio H_2O/N_2 ranging from 0 to 1.8 and for oxygen volume of 4% which is specific to MILD combustion regime. In order to characterize chemical effects of H_2O added to the oxidizer, an artificial inert species, F_H_2O, which has similar transport and thermodynamic characteristic injected. The difference between results with H_2O and F_H_2O is due to the chemical effects of added H_2O. The temperature is considerably reduced by H_2O chemical effect for a volume of 4% of oxygen, but when this later increased to 10% the temperature is slightly affected by H_2O chemical effect.

Figure 10(a) illustrates the thermal and chemical effects of water vapor on OH maximal mole fraction. This radical is reduced by both thermal and chemical effects of H_2O addition which are very important for the case with 10% oxygen and negligible in MILD regime when oxygen is about 4%. In this regime the maximum value of OH remains constant for all dilution percentages, whereas maximum value of OH is reduced by the combined thermal and chemical effect of H_2O.

The thermal and chemical effects on maximum CO (CO_{max}) value are presented in Fig. 10(b). The CO_{max} mole fraction is increased by chemical effects and reduced by thermal effects. Chemical effects are nearly constants for each value of oxygen volume contained in the oxidizer stream.

The maximum mole fraction of C_2H_2 species is significantly affected by the increase of oxygen, chemical effect of water vapor reduces this species, this reduction is more important with water vapor increasing in the air. MILD regime is characterized by low oxygen contained in the oxidizer, the C_2H_2 is significantly reduced by the thermal effects and slightly affected by chemical ones.

The thermal and chemical effects of H_2O addition on NO production are illustrated in Fig. 10(d) for the two cases of 4% and 10% oxygen in the oxidizer stream. In MILD combustion (4% oxygen), both effects are negligible whereas in the near conventional regime (10% of oxygen) the effects are visible and reduce the NO production especially when the water vapor increases in the oxidizer.

5. CONCLUSION

This study presents the effects of dilution by water vapor on the hydrogenated biogas MILD combustion. Water vapor content in the combustion air is characterized by the ratio H_2O/N_2 which is varied from 0 to 1.72 and the oxygen ranges from 4 % à 10 % in the oxidizer which is preheated at

1200K. Moreover, the fuel is enriched with a volume of 0 % to 30 % of hydrogen and injected at 300K. Pressure and strain rate are kept constant and respectively equal to 1 atm and 120 s^{-1}. The following conclusions can be deduced:

a) In flameless regime, the heat released by combustion is lower than that produced in conventional combustion mode, this reduces significantly emissions.

b) Oxygen reduction in the MILD combustion mode reduces temperature and all emissions.

c) The considered biogas didn't burn when the volume of oxygen is 4% until adding hydrogen which reactivated the mixture.

d) Oxygen increasing in the oxidizer breaks down the MILD regime and increases temperature and emissions.

e) Temperature is highly affected by the chemical and thermal effects of H_2O in a flameless regime, whereas in the conventional combustion it is only affected by the thermal effect.

f) The OH and CO species are strongly affected by chemical effects of H_2O in both flameless and conventional combustion modes.

g) Combined effects of H_2O on the production of the pollutants species C_2H_2 and NO are negligible in flameless combustion.

REFERENCES

CHEMKIN-PRO 15131 (2013), Reaction Design: San Diego.

Chernov, V., M. J. Thomson, S. B. Dworkin, N. A. Slavinskaya and U. Riede (2014). Soot formation with C1 and C2 fuels using an improved chemical mechanism for PAH growth. *Combustion and Flame* 161, 592-601.

De Joannon, M., P.Sabia, G.Cozzolino, G. Sorrentino and A. Cavaliere (2012a). Pyrolitic and Oxidative Structures in Hot Oxidant Diluted Oxidant (HODO) MILD Combustion, *Combustion Science and Technology* 84, 1207–1218.

De Joannon, M., P. Sabia, G. Sorrentino and A. Cavaliere (2009). Numerical study of mild combustion in hot diluted diffusion ignition (HDDI) regime. *Proceedings of the Combustion Institute* 32, 3147-3154.

De Joannon, M., G. Sorrentino and A.Cavaliere (2012b). MILD combustion in diffusion-controlled regimes of Hot Diluted Fuel, *Combustion and Flame* 159, 1832–1839.

Derudi, M., A. Villani and R. Rota (2007). Sustainability of mild combustion of hydrogen-containing hybrid fuels. *Proceedings of the Combustion Institute* 31, 3393-3400.

Fisher, E. M., B. A. Williams and J. W. Fleming (1997). Determination of the Strain in Counter flow Diffusion Flames From Flow Conditions. *Proceedings of the Eastern States Section of the Combustion Institute* 191-194.

Fuse, R., H. Kobayashi, Y. Ju, K. Maruta and T. Nioka (2002). NOx emission from high temperature air/methane counterflow diffusion flame. *International Journal of Thermal Sciences* 41,693–698.

Galletti.A, Parente.A, Derudi.M, Rota.R and Tognotti.L,(2009), Numerical and experimental analysis of NO emissions from a lab-scale burner fed with hydrogen-enriched fuels and operating in MILD combustion, *international journal of hydrogen energy* 34, 8339– 8351.

Glarborga, P., M. U. Alzuetab, K. Kjærgaarda and K. Dam-Johansena (2003). Oxidation of formaldehyde and its interaction with nitric oxide in a flow reactor. *Combustion and Flame* 132, 629–638.

Hadef, A., A. Mameri, F. Tabet and Z. Aouachria (2018). Effect of the addition of H_2 and H_2O on the polluting species in a counter-flow diffusion flame of biogas in flameless regime. *International Journal of Hydrogen Energy* 3475-3481

Hamdi.M., B.Hmaeid and M.Sassi (2009). Numerical modeling of the effects of fuel dilution and strain rate on reaction zone structure and NOx formation in flameless combustion, *Combusion Science and Techologie* 181,1078–1091.

Hinton.N and R.Ston (2014). Laminar burning velocity measurements of methane and carbon dioxide mixtures (biogas) over wide ranging temperatures and pressures, *Fuel*,116,743–750.

Hwang, D. J., J. W. Choi, J. Park, S. I. Keel, C. B. Ch. and D. S. Noh (2004). Numerical study on flame structure and NO formation in CH4–O2–N2 counter flow diffusion flame diluted with H_2O. *Int. J. Energy Res* 28, 1255–1267.

Kee, R. J., J. A. Miller and G. H. Evans (1988). Computational model of the structure and extinction of straind, opposed flow, premixed methane-air flames. *Twenty-Second Symposium (International) on Combustion*, The Combustion Institute 1479-1494.

Liu, F. S., H. S. Guo, G.J. Smallwood and O.L. Gulder (2001). The chemical effects of carbon dioxide as an additive in an ethylene diffusion flame: implications for soot and NO_x formation. *Combustion and Flame* 125, 778-787.

Liu, D., J. Santner, C. Togb, D. Felsmann, J. Koppmann and J. Lackner (2014). Flame structure and kinetic studies of carbon dioxide-diluted dimethyl ether flames at reduced and elevated pressures. *Combustion and Flame* 160, 2654–2668.

Mameri, A., F. Tabet and A. Hadef (2018). MILD combustion of hydrogenated biogas under

several operating conditions in an opposed jet configuration. *International Journal of Hydrogen Energy* 43,3566-3576.

Mameri, A. and F. Tabet (2016). Numerical investigation of counter-flow diffusion flame of biogase hydrogen blends: Effects of biogas composition, hydrogen enrichment and scalar dissipation rate on flame structure and emissions. *International journal of hydrogen energy* 41, 2011–2022.

Maruta, K., K. Muso, K. Takeda and T. Nioka (2000). Reaction zone structure in flameless combustion. *Proceedings of the Combustion Institute* 28, 2117–2123.

Park, J., D.S. Bae, M.S. Cha, J.H. Yun, S.I. Keel and H.C. Cho (2008). Flame characteristics in H2/CO synthetic gas diffusion flames diluted with CO2: effects of radiative heat loss and mixture composition. *International Journal of Hydrogen Energy* 33, 7256-7264.

Ruiz. M. P., A. Callejas, A. Millera, M. U. Alzueta and R. Bilbao (2007). Soot formation from C2H2 and C2H4 pyrolysis at different temperatures. *Journal of Analytical and Applied Pyrolysis*79, 244–251.

Seungro, L., P. Rosa, D-R. Derek, P. Trinh and K. Oh Chae (2015), Extinction limits and structure of counterflow non premixed H_2O-laden CH4/air flames. *Energy* 93, 442-450.

Sheng, C. and Z. Chuguang (2011). Counterflow diffusion flame of hydrogen-enriched biogas under MILD oxy-fuel condition. *International Journal of Hydrogen Energy* 36,15403-15413.

Smith, G. P., D. M. Golden, M. Frenklach, N. W. Moriarty, B. Eiteneer, M. Goldenberg, C. T. Bowman, R. K. Hanson, S. Song, J. W.C. Gardiner, V.V. Lissianski and Z. Qin (2000).

Sung, C. J., J. B. Liu and C. K. Law (1995). Structural Response of Counter flow Diffusion Flames to Strain Rate Variations. *Combustion and Flame* 102, 481-492.

Wunning.J (1991), Flammenlose Oxydation von Brennstoff mit hochvorgewärmter Luft, *Chemie Ingenieur Technik* 63,1243–1245.